Journal of Hydrology: Regional Studies 56 (2024) 102058

Contents lists available at ScienceDirect

Journal of Hydrology: Regional Studies

journal homepage: www.elsevier.com/locate/ejrh

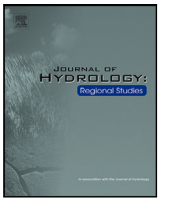

Regional-scale seasonal forecast of surface water availability in a semi-arid environment: The case of Ceará State in Northeast of Brazil

Erwin Rottler [a,b,c,*], Martin Schüttig [b,c], Axel Bronstert [b,c], Alyson Brayner Sousa Estácio [d], Renan Vieira Rocha [d], Valdenor Nilo de Carvalho Junior [d], Clecia Cristina Barbosa Guimarães [d], Eduardo Sávio P.R. Martins [d], Christof Lorenz [e], Klaus Vormoor [b,c]

[a] *Department of Geography, University of Innsbruck, Innrain 52f, Innsbruck, 6020, Tyrol, Austria*
[b] *Institute of Environmental Science and Geography, University of Potsdam, Karl-Liebknecht-Str. 24–25, Potsdam, 14476, Brandenburg, Germany*
[c] *UP Transfer GmbH, Am Kanal 47, Potsdam, 14467, Brandenburg, Germany*
[d] *Ceará Institute for Meteorology and Water Resources (FUNCEME), Avenida Rui Barbosa 1246, Fortaleza, 60001, Ceará, Brazil*
[e] *Institute of Meteorology and Climate Research - Atmospheric Environmental Research (IMK-IFU), Karlsruhe Institute of Technology, Kreuzeckbahnstr. 19, Garmisch-Partenkirchen, 82467, Bavaria, Germany*

ARTICLE INFO

Keywords:
Data assimilation
Remote sensing
Seasonal forecast
Semi-arid
Water availability

ABSTRACT

Study region: Ceará (Brazil).
Study focus: Considerable intra- and inter-annual variability of rainfall in this semi-arid region lead to strong temporal variations in water availability. To store and supply water in times of water scarcity, tens of thousands of freshwater reservoirs have been built over time, most of which are unmonitored. Here, we develop a hydrological forecasting system for the entire state of Ceará which integrates satellite-based monitoring of reservoir water storage, bias-corrected seasonal weather forecasts and hydrological modeling of freshwater availability. We test and demonstrate the applicability of this system by conducting experiments with historic data, hindcasts and forecasts.
New hydrological insights for the region: The assimilation of in-situ and Sentinel-1 based observations of reservoir fillings into the hydrological model WASA-SED proved to be feasible and an important step in the modeling of available water resources dynamics. Hydrological simulations for January to June from 1990–2019 based on meteorological observations resulted in a median average NRMSE between observed and modeled reservoir fillings of strategic reservoirs of 29.51%. The comparison of observed and predicted precipitation from two different seasonal forecasting systems were in the same order of magnitude (i.e. 19.51% and 24.52%). Hindcast experiments suggested the superposition of uncertainties of different model components. Efforts are currently being made to further test and improve the developed integrated framework as part of the operational service.

* Corresponding author at: Department of Geography, University of Innsbruck, Innrain 52f, Innsbruck, 6020, Tyrol, Austria.
E-mail address: erwin.rottler@uibk.ac.at (E. Rottler).

https://doi.org/10.1016/j.ejrh.2024.102058
Received 15 May 2024; Received in revised form 31 October 2024; Accepted 2 November 2024
Available online 8 November 2024

1. Introduction

Droughts and uncertain water supply threaten the livelihood of people in many dryland regions of the world. Increasing water demand and climatic changes have the potential to further aggravate the situation by intensifying drought events and their socio-economicimpact (Trenberth et al., 2014; Marengo et al., 2017; Liu et al., 2018; Raulino et al., 2021; Vogel et al., 2021; Yuan et al., 2023). In many cases, strong inter- and intra-annual variability in precipitation pose a key challenge for local water agencies to secure the water supply for the multitude of needs and utilizations including the provision of drinking water for the local population, irrigation in the agricultural sector, preservation of (aquatic) biotopes and water for industrial processes (Rossi and Cancelliere, 2013; Marengo et al., 2017; Sugg et al., 2020; Naumann et al., 2021).

A region well known for such conditions is the Northeast of Brazil, where the so-called drought polygon comprises a region of about 750 000 km^2 (Marengo and Bernasconi, 2015; Meira Neto et al., 2024). One prominent example in this north-eastern region of Brazil is the state of Ceará. Thousands of reservoirs of highly variable sizes have been built since the 19th century to manage freshwater and cope with the water scarcity challenges (Pereira et al., 2019; Mady et al., 2020). The control of the reservoirs and its networks, including water diversions, enables communities and municipalities to manage the spatio-temporal distribution of water. Good reservoir management strategies can lower drought impacts and in turn foster social stability and livability (Campos and Studart, 2000; Formiga-Johnsson and Kemper, 2005; Campos and Studart, 2006; de Araújo et al., 2018, 2023).

However, a good water management is in need of a variety of information on the hydro-meteorological conditions. An extensive operational monitoring network capturing the current state of the water resources commonly forms the backbone of any beneficial water management. Because of the huge overall number of reservoirs in Ceará, however, only a selection of strategic reservoirs are systematically monitored and managed (Pilz et al., 2019; Meira Neto et al., 2024). The vast majority of (mostly small to medium sized) reservoirs lack a systematic control and are managed only locally. No information on water volumes stored on those unmonitored reservoirs is available at the state level (Mamede et al., 2012; Pereira et al., 2019). In recent years, remote sensing based approaches have been tested to overcome this issue. Satellite data inter alia has been harnessed to investigate the dynamics of chlorophyll-a and colored dissolved organic matter (Coelho et al., 2017), terrain and shape attributes (Pereira et al., 2019), the bathymetry (Zhang et al., 2016, 2021; Bacalhau et al., 2022; Duplančić Leder et al., 2023), the water surface extent (Huang et al., 2018; Zhang et al., 2021) and the evaporation (Rodrigues et al., 2021, 2024) from reservoirs. In-situ and satellite-based monitoring can be complemented by seasonal forecasting systems, which provide information on the water availability for the upcoming months (Souza Filho and Lall, 2003; Pilz et al., 2019; Costa et al., 2021). Recent research points at the potential of new seasonal forecasting products and bias adjustment techniques to support the water management in dryland regions (Hao et al., 2018; Delgado et al., 2018; Bürger, 2020; Lorenz et al., 2021; Portele et al., 2021; Borne et al., 2022).

In this study, we aim to develop an integrated system for the monitoring and forecasting of hydrological dynamics for the state area of Ceará, Brazil. We base our system on an integrated use of (i) satellite-based water surface monitoring, which provides, in combination with satellite-derived bathymetries, information on current water storage within reservoirs, (ii) bias-corrected seasonal weather predictions from two different sources and (iii) physically-based hydrological model simulations (Fig. 1). The in-situ measured and remotely sensed information on reservoir fillings is assimilated into the hydrological model. Seasonal weather predictions originate from a seasonal forecast system operated by the Research Institute for Meteorology and Water Resources, Ceará, Brazil (FUNCEME) using the climate model ECHAM4.6 (Roeckner et al., 1996; Sun et al., 2006) and the long-range seasonal forecasting system SEAS5 from the European Centre for Medium-Range Weather Forecasts (ECMWF) (Stockdale et al., 2018). The hydrological simulations are based on the hydrological model WASA-SED (Water Availability in Semi-Arid environments - SEDiments) (Güntner, 2002; Güntner and Bronstert, 2004; Mueller et al., 2010; Bronstert et al., 2014). The overall research question is how well an integrated monitoring and modeling system can predict the seasonal water availability in the complex dryland environment of Ceará. In view of the overall goal, we aim to identify, collect and process required data, assess the performance of the modeling chain components and the system as a whole, discuss sources of uncertainty and shortcomings of the modeling chain, gain new hydrological insights with regard to the reservoir network for the region and draft possible advancements of the established structures.

2. Materials and methods

2.1. Study area

The state of Ceará is located in the semi-arid north-east of Brazil (Fig. 2). It covers an area of about 146 500 km^2 and an elevation range from sea level to approximately 1100 m. Ceará is characterized by a tropical savanna climate, which signifies high monthly and annual average temperatures and strong inter- and intra-annual rainfall variability, with the largest rainfall amounts occurring during the rainy season from January to May (Frischkorn et al., 2003). The region is considered to be among the most densely populated dryland areas in the world (Marengo et al., 2017) and a vulnerable water supply exposes large parts of the population to the effects of droughts (Marengo et al., 2022; de Andrade et al., 2016; de Araújo and Bronstert, 2016; Chimeli et al., 2008). Several severe drought situations have been documented throughout time. The last severe drought occurred from 2012 to 2018 (Pontes Filho et al., 2020).

In order to mitigate the impacts of droughts and to ensure water supply during the dry season, Ceará is pervaded by a water storage system comprising tens of thousands of reservoirs and various large scale water diversions (van Oel et al., 2008). At the time of this study, Ceará's state water resources company COGERH operates 157 of these reservoirs. Only these so-called strategic

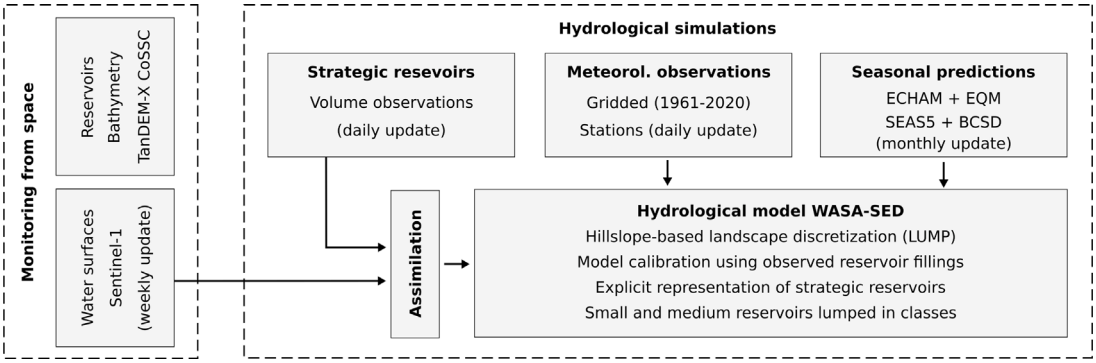

Fig. 1. Scheme of the analytical set-up depicting the key components of the forecasting system integrating satellite-based monitoring, seasonal weather predictions and hydrological modeling.

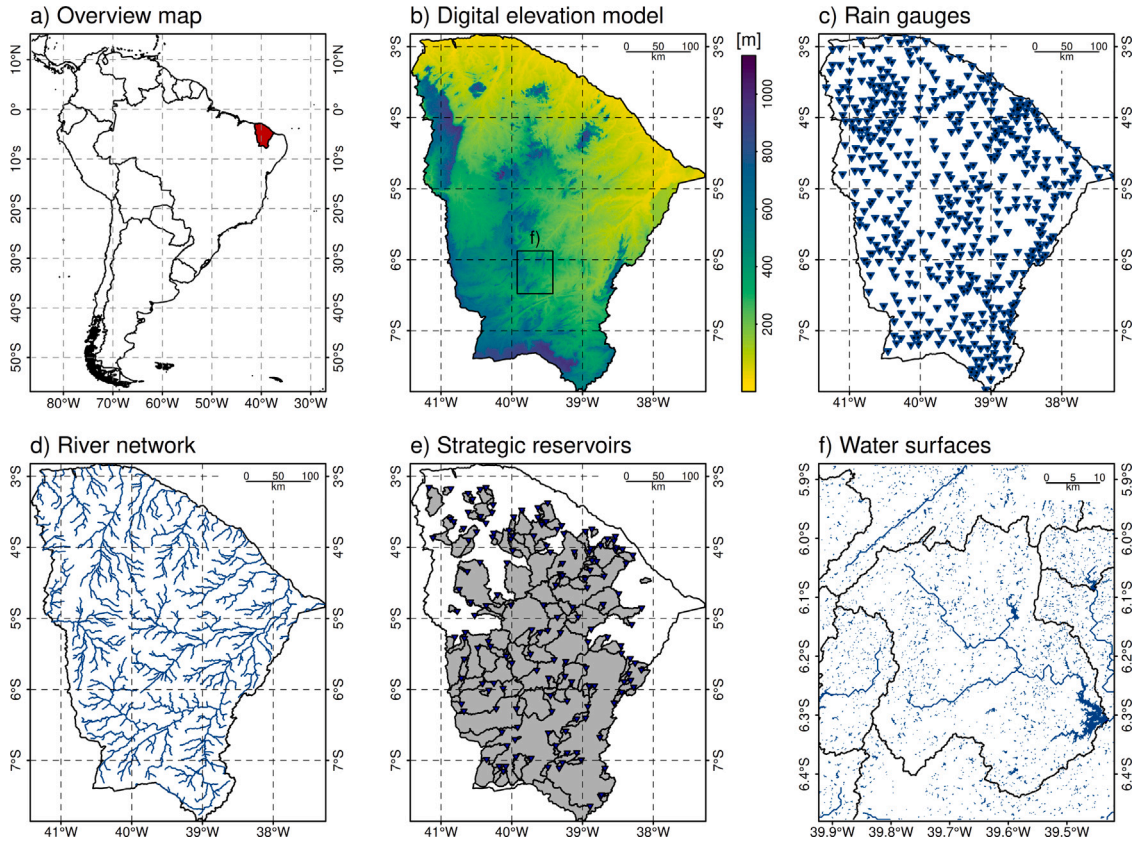

Fig. 2. Location of the state of Ceará within South America and Brazil (a), digital elevation model (b), locations of rain gauges (c), river network (d), location and watersheds of strategic reservoirs (e) and a detailed view on the strategic reservoir Trussu (id = 122) showing water surfaces, river network and watershed boundaries (f). The location and extent of the area in panel f is indicated with a black box in panel b.

reservoirs have a known bathymetry, are operationally monitored and are subject to systematic water management. State authorities continuously work on increasing the number of strategic reservoirs. The vast majority of reservoirs are not systematically controlled and managed only locally. A detailed view on the watershed of the strategic reservoir Trussu provides insights into the density of this network of small reservoirs (Fig. 2f).

2.2. Data

2.2.1. Reservoir monitoring from space

Satellite-based surveys conducted by FUNCEME provide information on water surface features and their locations in Ceará for the years 2008, 2009, 2011, 2013, 2014, 2015, 2016, 2017 and 2020 (Funceme, 2020). A step-by-step overlay of all detected water surfaces results in the maximum observed extent of the water surface observed for the investigated years. After removing river segments and coastal wetlands, a total of 57 247 water surface features remain. All features together cover a total area of 3553.78 km^2, whereby 1534.79 km^2 (43.19%) are water surfaces areas of the 155 strategic reservoirs and 2018.99 km^2 (56.82%) are other water surfaces.

The extent of these features is considered the maximum extent of lake and reservoir surfaces for the satellite-based derivation of the bathymetry and water surfaces (see Section 2.3.1). The observed satellite-based maximum extents for strategic reservoirs can be compared to potential maximum geometries provided by COGERH. The comparison shows that the observed maximum extents are smaller than potential maximum extents (on median average 44.2%).

Bathymetric information is derived for a large number of unmonitored reservoirs from high-resolution digital elevation models (DEMs). We used TanDEM-X (TerraSAR-X add-on for Digital Elevation Measurement) CoSSC (Coregistered Single look Slant range Complex) data to generate these DEMs (Fig. 1). Specifically, we used scenes acquired in stripmap mode. The resolution is around 3 m × 1 m to 2 m (azimuth × slant range), depending on the actual acquisition conditions and processor settings. The TanDEM-X radar satellite mission has been launched in 2010 and operated by DLR with the goal to generate a consistent, high-resolution DEM with worldwide coverage (Krieger et al., 2007; Rizzoli et al., 2017). This product, however, cannot be directly used as water areas are masked out in the global DEM. For appropriate bathymetric information to be derived, we selected and processed TanDEM-X CoSSC scenes which meet the following criteria: (i) scenes need to be acquired during the dry season (August to December), and (ii) scenes need to be acquired after the onset of the latest drought period (2012) and ideally cover one of the two driest years 2015 and 2016, however, do not exceed the end of the drought period (2019). Based on these criteria, it can be assumed that the water levels in the reservoirs were very low to completely dry. Applying these criteria to the TanDEM-X catalogue results in a set of 59 scenes which cover 27 794 reservoirs (48% of the reservoir inventory used in this study). The data can be downloaded upon request via the EOWEB GeoPortal (https://eoweb.dlr.de/egp/).

Sentinel-1 data (Level 1 GRD) is available at the Copernicus Open Access Hub via their API and utilized to derive the temporal and spatial water extent of the reservoirs. Over land, Sentinel-1 data is primarily obtained in Interferometric Wide Swath (IW) mode. The high resolution dataset results in a pixel spacing of 10 × 10 m. Both Sentinel 1A and 1B have a revisit time of 12 days. New data is constantly processed to monitor water surfaces within the reservoirs. Data is available since spring 2015, with seven to eight new scenes added every week for the state of Ceará, so that more than 2200 scenes are available for this study.

2.2.2. Hydrological simulations

A network of stations provides meteorological observations for Ceará. In this study, we use daily resolution station-based measurements of temperature, precipitation, relative humidity and solar radiation. Historic data sets of station observations were provided by FUNCEME. With regard to precipitation, the state of Ceará maintains a dense network of stations dating back to the 1970s. We updated precipitation data from 543 rain gauges (Fig. 2c). However, other meteorological variables are measured at less sites across the state and only in recent years. In order to have temperature, relative humidity and radiation input data for hydrological simulations dating back to the 1980s, we use historic information from the daily gridded weather data for Brazil by Xavier et al. (2022).

With regard to the strategic reservoirs, data was available for 155 (out of 157) strategic reservoirs in the state of Ceará (Fig. 2e). Two strategic reservoirs were only very recently incorporated into the system. For those 155 reservoirs, an official water-level–lake-area–storage-volume relationship and in-situ observations of the water storage volume are available. Historic time series of daily resolution storage volumes were provided by FUNCEME. Updated times series can be obtained via the FUNCEME API (http://api.funceme.br/). It is worth to note that bathymetric information often stem from the date of reservoir installation and that any possible changes, e.g. by sediment deposition, are not included. Information on the spillway level, parameters of the spillway rating curve and watershed boundaries of the strategic reservoirs were provided by FUNCEME and COGERH. Observational data on the controlled outflow from the strategic reservoirs is also available. The 155 strategic reservoirs used in this study have a total storage capacity of 18 622.54 hm^3. Between 1958 and 1966 the construction of several large reservoirs (i.e., Araras in 1958 with 860 hm^3, Oros in 1962 with 1940 hm^3 and Banabuiú in 1966 with 1601 hm^3) resulted in a strong increase in monitored storage capacity. The constructions of the by far largest strategic reservoir, i.e. Castanhão, having a storage capacity of 6700 hm^3 was completed in 2002. Those four largest reservoirs represent about 60% of the total monitored reservoir volume. 112 out of the 155 strategic reservoirs have a capacity below 50 hm^3 and represent 9% of the total observed strategic storage capacity. The monitoring of most strategic reservoirs started in the 1980s.

For the hillslope-based landscape discretization, we process spatial information on the topography, soil types and land cover. The SRTM digital DEM was provided by the International Centre for Tropical Agriculture (Reuter et al., 2007; Jarvis et al., 2008). The soil map along with soil parameters from a local database (Jacomine et al., 1973) were provided by FUNCEME. With regard to soil parameter required in the hydrological model, we use the set of parameters compiled by Pilz et al. (2019). With regard to land cover, we use the map from the Brazilian Ministry of the Environment along with parameters assembled by Güntner (2002). In total, we distinguish 16 soil types and 34 land cover types. All input maps have a common spatial resolution of approximately 90 m.

Information on small reservoirs base on the same reservoir surface data set used within the satellite-based water surface monitoring (see Section 2.2.1).

We force the hydrological model WASA-SED with seasonal forecast data from two sources. On the one hand, we use data originating from ECHAM4.6 general circulation model runs conducted at FUNCEME. The ECHAM forecasting system at FUNCEME is in operational use and new forecasts with 20 ensemble members are available on a monthly basis. In addition to the current forecasts, we use ECHAM hindcast simulations dating back to the 1990s. We bias correct precipitation and temperature data from the ECHAM model by means of empirical quantile mapping (EQM; Gudmundsson et al. (2012)) with reference to the station network. Further forcing variables for the hydrological model (i.e. solar radiation and relative humidity) are directly taken from ECHAM without further treatment. On the other hand, we conduct hydrological simulations based on the fifth generation of ECMWF's seasonal forecasting system SEAS5 (Stockdale et al., 2018; Johnson et al., 2019). SEAS5 is in operational use and running with 51 ensemble members since November 2017. Hindcast data with 25 ensemble members is available from 1981 to 2016. SEAS5 is a state-of-the-art seasonal forecast system and is widely evaluated and used (Gubler et al., 2020; Crespi et al., 2021; Ferreira et al., 2022). We correct the SEAS5 data for biases and model drift by applying a bias-correction and spatial-disaggregations (BCSD) approach using ERA-Land data as a Ref. Lorenz et al. (2021).

2.3. Methods

2.3.1. Monitoring surface water resources from space

To derive the area-volume relationships (AV-curves) for the unmonitored reservoirs, the TanDEM-X CoSSC scenes are processed to DEMs with approximately 10 × 10 m spatial resolution using the freely available SeNtinel Application Platform (SNAP; version 8.0) and the installed plugin 'snaphu'. The processing follows the workflow described in Zhang et al. (2016) and includes interferometry generation, phase filtering, multi-looking, unwrapping, and phase-to-height conversion. The resulting DEMs are masked by the maximum reservoir extents (i.e. polygons) and the bathymetry of each reservoir is estimated at a vertical distance of 0.5 m. This way, AV-curves have be derived for all reservoirs covered by the TanDEM-X scenes, i.e. 27 794 reservoirs (see 2.2.1).

For the remaining 29 964 reservoirs, we regionalize AV-curves from the covered reservoirs based on physiographic similarity. We have tested various (combinations of) predictors like geological region, size (i.e. maximum reservoir extent), and polygon shape, with size as the single predictor proving most effective (Pearson correlation coefficient of 0.84). Thus, we have classified the reservoirs with AV-curves into five equal groups, each with the same number of members (i.e. 5 559). For each group, a representative AV-curve is estimated. That is, the median number of vertical steps is identified, and for each vertical step the median area and volume is derived from the original AV-curves per group. Depending on the size of an uncovered reservoir, the corresponding representative curve is then assigned.

The quality of the AV-curves can only be assessed for the strategic reservoirs that are fully covered by the selected TanDEM-X scenes and which were empty (<0.5 m water level) at the recording date of the particular TanDEM-X scene. Thus, only 34 of the 155 strategic reservoirs can be used for this comparison. We evaluate our AV-curves against the official curves from COGERH based on the Mean Absolute Percentage Error (MAPE):

$$MAPE = \frac{1}{n}\sum_{i=1}^{n}\frac{|x_i - y_i|}{y_i} \times 100\%$$

where x_i is the water volume derived from the processed DEM for a specific water area and y_i is the volume derived from official AV relationship for the same water area. In areas where scenes are overlapping or recorded at different valid dates, we can also compare different curves for the same reservoir. For one specific example reservoir (i.e. Torado - Bacia Banabuiú), which has also been used by Zhang et al. (2016), we compare different curves with each other and against official COGERH data to get an impression of the influence of the recording date on the quality of AV-curves.

Water areas within reservoirs are detected by classifying the backscatter (in dB) of Sentinel-1 images based on a bimodal distribution of pixel values (water, no-water). The preprocessing of Sentinel-1 images follows the generic workflow presented by Filipponi (2019) and applies a series of standard corrections, a precise orbit acquisition, the removal of thermal and image noise, a radiometrical calibration, a range Doppler terrain correction, and the conversion of unitless backscatter to dB. For the distinction between water and no-water areas, we apply the simple, nonparametric and unsupervised threshold approach introduced by Otsu (1979). This method optimizes the threshold to be used for the classification by maximizing the variance between two classes of pixels. Therefore, this approach assumes bimodality in the histogram of pixel values which might not always be the case (e.g. Markert et al., 2020). To overcome this issue, we apply a region-growing image segmentation (seed value −16 dB) for the extent of the maximum lake area which yields in bimodally distributed pixel values. Otsu's method is then applied to this histogram for each reservoir individually.

To assess the quality of the derived watermasks, observed areas of the strategic reservoirs (inferred from water levels and official AV-curves) are compared with the estimated watermask areas. The time period for the assessment covers the years 2015 to 2022. The performance is then evaluated by means of the symmetrical mean absolute percentage error (SMAPE):

$$SMAPE = \frac{1}{n}\sum_{i=1}^{n}\frac{|x_i - y_i|}{(|x_i| + |y_i|)} \times 100\%$$

where x_i is the area of the derived watermask and y_i is the area calculated from measurements with the official AV-relationship. Note, that we refuse to divide the sum in the denominator by two since a percentage error between 0% and 100% is easier to interpret.

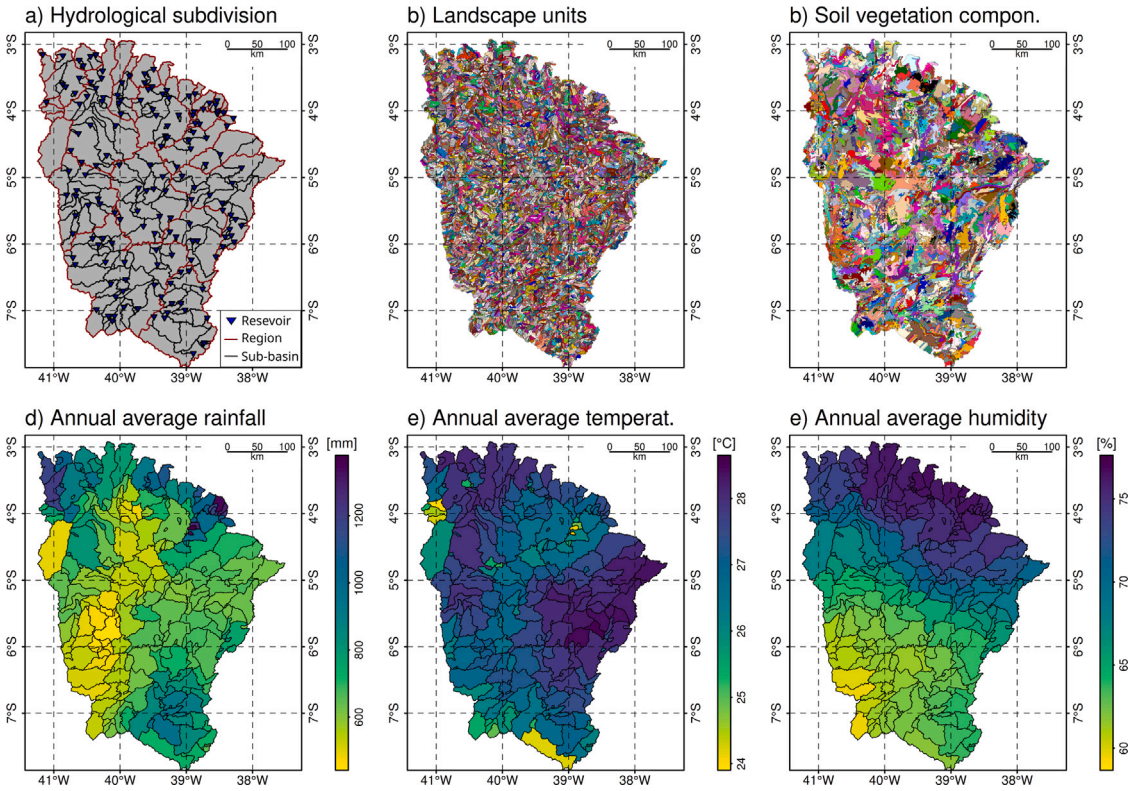

Fig. 3. Hydrological subdivision of the study area (a), elementary hillslopes units and their grouping into landscape units (LUS; b), soil vegetation components (SVCs; c) and long-term annual averages (1990–2019) of precipitation, temperature and relative humidity resulting from the interpolation of observations to sub-basin level (d, e and f). LUs (93) and SVCs (445) are displayed with random colors. (For interpretation of the references to color in this figure legend, the reader is referred to the web version of this article.)

2.3.2. Hydrological simulations

WASA-SED is a spatially semi-distributed and hillslope-based hydrological model, specifically designed to assess water availability and sediment transport in semi-arid regions (Güntner, 2002; Güntner and Bronstert, 2004; Mueller et al., 2010; Bronstert et al., 2014). In contrast to the Soil and Water Assessment Tool (SWAT) model or the Automated Geospatial Watershed Assessment (AGWA) model, the landscape discretization in WASA-SED is hillslope-based and allows for the preservation of the landscape variability and a more detailed modeling of overland flow. The possibility to represent storage reservoirs in WASA-SED explicitly (large and strategic reservoirs) and in an aggregated way (small to medium sized reservoirs) enables the incorporation and efficient modeling of the large number of reservoirs in Ceará as well as the assimilation of observed filling levels from all reservoir types. As the model is developed within the working group of the authors, insightful experiences in its application and performance were available from the very beginning of the study. We use the R package lumpR for the hillslope-based landscape discretization of the study area (Pilz et al., 2017). This R package is tailored to the needs of WASA-SED and provides easy access to the algorithms of the software tool LUMP (Landscape Unit Mapping Tool) (Francke et al., 2008).

In the process of the landscape discretization, we sub-divide the study area into hydrological regions and sub-basins. Strategic reservoirs are always located at the outlet of a sub-basin. The model set-up for Ceará is sub-divided into 28 regions and 263 sub-basins (Fig. 3a). Furthermore, we discretize the entire area into elementary hillslope units and group the representative hillslope profiles into 93 landscape units (LUs), which are partitioned into three terrain components (Fig. 3b). The overlay of soil and land cover maps results in 445 soil vegetation components (Fig. 3c), whose areal fractions within each TC of each LU are calculated. Small and medium sized reservoirs are included into WASA-SED in an aggregated way, grouping them into five classes according to their size. For each sub-basin and reservoir class the water balance of a hypothetical representative reservoir with mean characteristics is calculated (Güntner, 2002; Güntner and Bronstert, 2004; Mueller et al., 2010). The area-volume relationships of the representative reservoirs of each class are by default defined using empirical approach by Molle (1994). We interpolate meteorological input on sub-basin level (the level of the meteorological input of the hydrological model) using inverse distance weighting (IDW) from the R package geostat (Kneis, 2012). Long-term averages (1990–2019) of annual precipitation, temperature and relative humidity are presented in Fig. 3d–f.

In this study, we apply a region-specific calibration approach. Hence, every region gets its own set of parameters. Following the work of Pilz et al. (2019), we use observed positive volume changes in the strategic reservoirs, which effectively is caused by runoff

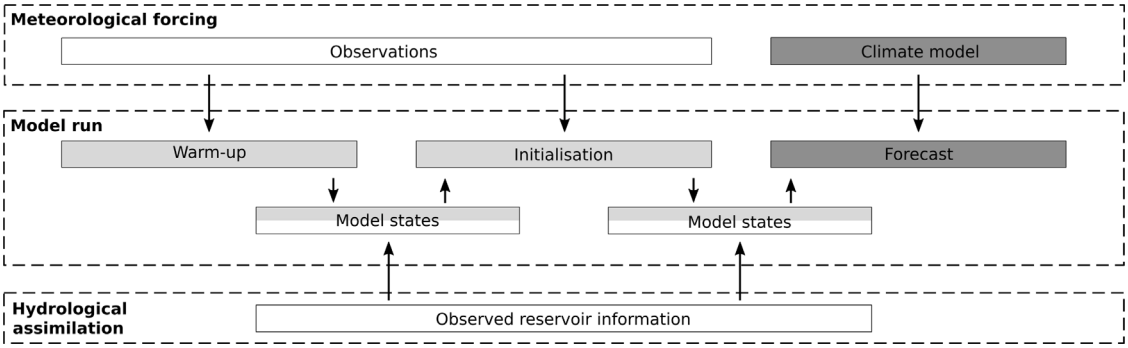

Fig. 4. Scheme of the forecast model set-up with the assimilation of observed reservoir information via the update of exported model states.

draining into the reservoirs, as target variable. Streamflow measurements are available for selected river segments in the region, however, large uncertainties are induced into the highly variable streamflow inter alia by broad and dynamic cross sections and dense riparian vegetation. In contrast to Pilz et al. (2019), who only uses the positive volume changes in the strategic reservoir at the outlet of a region, we incorporate observations of all strategic reservoirs enclosed into a region (multi-reservoir calibration). To account for the wide range of reservoir sizes and therefore varying importance for the water balance within a region, we further refine the approach and conduct a region-specific and capacity-weighted model calibrations. After each model run, we calculate the Percentage Bias (PB) (e.g., Yapo et al., 1996) between observed and simulated positive volume changes and assess the average PB for the region weighted according to the capacity of the strategic reservoirs. The capacity-weighted multi-reservoir approach enables us to incorporate information from all strategic reservoirs into the calibration process and to calibrate regions that do not have a strategic reservoir at the outlet.

We carry out the calibration by using the dynamically dimensioned search algorithm (Tolson and Shoemaker, 2007) from the R-package 'ppso'. In each calibration experiment, we conduct a minimum of 500 daily resolution model runs for the 20-year time frame 2000–2019. We concluded that for the present setting, a long calibration time frame that includes reservoir observations from multiple dry and wet years is required to get robust parameters. Using this approach, we adapt to the highly variable hydrological condition in the area and follow the recommendation by Shen et al. (2022) who point out that the commonly used split sample test framework usually is an 'inferior choice'. In total, we calibrate twelve parameters controlling interception, infiltration, percolation and groundwater processes. Parameters are either calibrated directly or in a multiplicative manner, i.e. model parameters are multiplied by a factor. For each parameter, we pre-define a value range that can be sampled by the calibration algorithm. In the case of the parameter specifying the root depth, for example, previously determined root depths for each vegetation type and season can be multiplied by a factor between 0.4 and 2. For regions without monitored strategic reservoirs, the transfer of calibrated parameter sets from neighboring regions was required. On average, the best performing model runs for the regions reach an absolute PB value of 11%.

To obtain the best possible starting point for the seasonal hydrological forecast, we assimilate in-situ volume observations from strategic reservoirs and satellite-based volume information on medium and small reservoirs. Observed volumes are assimilated directly via exported model states. In case no volume observation is available, the simulated value from the initialization run is used. With regard to satellite-based observations, we assess the average filling level of reservoirs of each class and sub-basin and assign this value to the representative reservoir simulated in the model. Prior to a hindcast/forecast run, we conduct a 3-year warm-up and a one-year initialization run to prepare to model storages for the simulation with seasonal forecast data (Fig. 4).

Our first simulation experiment with the assimilation of reservoir information consists of historic model runs based on observational meteorological data covering the time frame 1990–2019. At each model re-start in January, we assimilate exported model states from the previous year and update volumes from the strategic reservoirs with observations. As satellite-based data has only become available in recent years, we do not assimilate lumped volume information for the reservoir classes in this historic experiment. Next, we conduct hindcast experiments with data from the ECHAM and SEAS5 forecast systems. We conduct warm-up and initialization runs based on observations and subsequently force the hydrological model with hindcast data for the years 1990–2019. In this hindcast experiment, we focus on the wet season and only consider model runs starting in January of each year.

In a final step, we conduct hydrological simulations with current forecast data. In this case, the warm-up and initialization runs base on up-to-date station observations (no gridded products). In these forecast runs, we assimilate both volume information of strategic reservoirs based on in-situ measurements and satellite-based volume information for the reservoir classes. In this study, we exemplary show forecast results for the years 2019, 2020, 2021 and 2022 for the strategic reservoir Trussu (id = 122), which was constructed in the year 1996 and is located upstream the second largest strategic reservoir in Ceara (i.e. Oros) at a tributary of the Jaguaribe River (Fig. 2). We select this reservoir, as it has a comparatively large capacity (268.8 hm^3; 11th largest strategic reservoir in Ceará), does not have any other strategic reservoirs upstream and the reservoir watershed only consist of one sub-basin.

To track uncertainties along the modeling chain, we evaluate the performance of different components. First, we aim to evaluate the hydrological model and quantify its uncertainty by comparing simulated and observed reservoir volumes. We assume that the meteorological forcing based on observations can enable accurate simulations of reservoir volumes and that any difference between

and simulated and observed reservoir volumes is due to uncertainty within the hydrological model. Next, we assess the performance of the ECHAM and SEAS5 forecast systems by comparing cumulative precipitation sums from the hindcast simulations with observed values. In the following, we refer to the results of this assessment of precipitation input data as the uncertainty coming from the climate models. Finally, we assess the uncertainty of the full modeling chain by comparing predicted and observed volumes of the strategic reservoirs. In the hindcast experiments, the uncertainty coming from the climate forecast and the uncertainties of the hydrological model take effect. As a comparison, we also assess the performance of the long-term average of in-situ volume observations as prediction.

For the performance assessment, we assess the Kling-Gupta Efficiency with knowable-moments (KGEkm; Pizarro and Jorquera (2024)) and the Normalized Root Mean Square Error (NRMSE) between observed and simulated values. The KGEkm is a modification of the original Kling-Gupta efficiency (KGE; Gupta et al. (2009)) and was assessed in its default settings using the R package hydroGOF (Zambrano-Bigiarini, 2024) and daily resolution values. We calculate the NRMSE between observed and simulated values as follows:

$$NRMSE = \frac{\sqrt{\frac{1}{n}\sum_{i=1}^{n}(sim_i - obs_i)^2}}{\max(obs_1, \ldots, obs_n)}$$

where simulated (*sim*) and observed (*obs*) values are either monthly average values for reservoir volumes or cumulative monthly sums for precipitation (after the downscaling, bias-correction and interpolation to the sub-basin centroids) and n indicates the length of the prediction horizon, whereby n can be between 1 (January only) and 6 (January to June). The NRMSE provides a single measure of predictive power, which we can calculate for both reservoir volumes and cumulative precipitation. The normalization is necessary to enable the comparison between dry and wet years and between reservoirs of different sizes. We normalize by the maximum observed value during the prediction horizon. Hence, the NRMSE reflects the accuracy of the model per unit of available water in the reservoir or as precipitation during the prediction horizon. We assess the NRMSE for all reservoirs/sub-basins for the January forecast between 1990 and 2019 and for six prediction horizons with increasing length. Next, we either average all values of one reservoir/sub-basin, which results in a reservoir/sub-basin-specific performance estimation or we average the results from all reservoir/sub-basin from one year to get a performance estimate over time.

3. Results

3.1. Monitoring reservoirs from space

3.1.1. Area-volume relationships

The comparison of TanDEM-X derived AV-curves for the 34 strategic reservoirs with the official AV-curves from COGERH results in MAPE values ranging from 15.1% to 2 772% (76% without outliers) with a median value of 53.9% (Fig. 5a). Our results suggest that we systematically estimate lower reservoir volumes for the same lake area compared to the official curves from COGERH. There is no systematic spatial pattern recognizable with respect to the distribution of the MAPE values (Fig. 5a). Still, for no obvious reason, a cluster with particularly high error values is found in the north (Metropolitan Region Fortaleza). We also examined the relationship between the magnitude of the error and the size of the lake area, as well as the date of the TanDEM-X scene acquisition, but could not find any specific correlation.

The comparison of AV curves derived from scenes with different recording dates with COGERH data and the AV-curve from Zhang et al. (2016) (Fig. 6) shows (i) that the recording date of the scenes has an impact on the derived AV-curves (overestimation with the scene from Nov 2017; underestimation with two scenes from Nov 2015), and (ii) that the curves derived in this study from remotely sensed data only show a bit lesser agreement as the curve of Zhang et al. (2016), who also conducted ground-truthing and field surveys.

3.1.2. Water surface area detection

The remote sensing based watermask detection algorithm using Sentinel-1 data is evaluated for all 155 strategic reservoirs. SMAPE values range from 3.9% to 93.3% with a median of 22.6%, (Fig. 5b). The spatial distribution of the SMAPE shows no clear picture, though the largest derivations are found in the central sub-basins, while the dynamics are covered more accurately in the north and south.

3.2. Hydrological simulations

3.2.1. Role of different precipitation data and related uncertainty

In the framework of the hindcast experiments, we conduct hydrological simulations based on bias-corrected and downscaled SEAS5 and ECHAM data. Calculations of the NRMSE between cumulative monthly observed (and spatially interpolated) precipitation data and precipitation originating from the two forecasting systems for all 263 sub-basins of the hydrological model set-up result in a median average NRMSE of 19.51% for SEAS5 precipitation and a median average NRMSE of 24.52% for ECHAM precipitation for the prediction horizon January to June (Fig. 7a), which is the wet, hydrologically particular active season in the region. The prediction performance of the climate models referring precipitation seems homogeneous across the state of Ceará and no significant systematic spatial disparities show up (Fig. 8c,f).

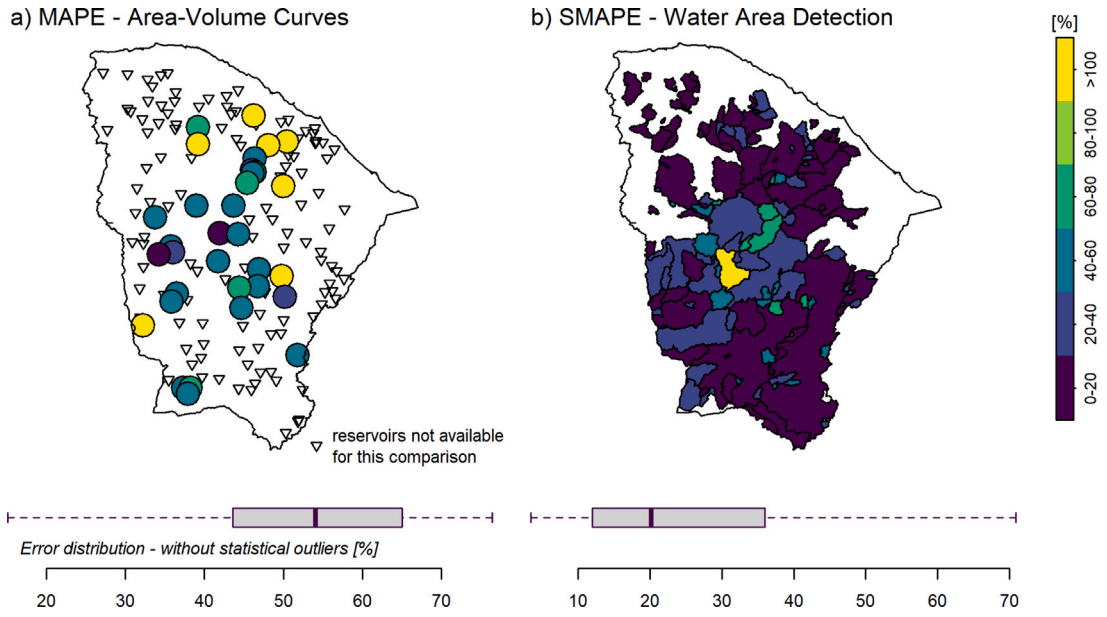

Fig. 5. (a) Mean absolute percentage error (MAPE) of the comparison between TanDEM-X derived- and official AV-curves provided by COGERH for 34 strategic reservoirs; (b) Symmetrical mean absolute percentage error (SMAPE) of the comparison between water areas as detected by remote sensing and official estimates from COGERH for 155 strategic reservoirs.

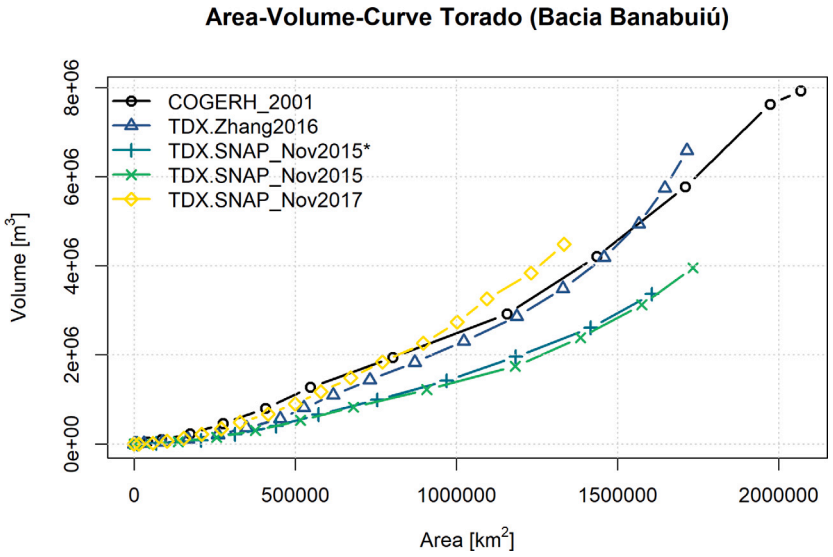

Fig. 6. AV-curves for one example reservoir derived from several TanDEM-X scenes taken at different dates as compared to the AV-curves from Zhang et al. (2016) and COGERH, respectively.

3.2.2. Simulations of reservoir water dynamics

Yearly hydrological simulations for January to June from 1990–2019 based on historical observations result in a median average NRMSE for all strategic reservoirs of 29.51% (Fig. 7a). In other words, when forcing the WASA-SED set-up for Ceará with observed meteorological data, an "average" simulated reservoir volume in Ceará has a mean error of 29.51%. The model performance strongly varies from reservoir to reservoir (Fig. 8a). According to our analysis, 44 out of the 155 strategic reservoirs (approx. 28%) have an average NRMSE below 20%. The best performing reservoirs are located in the southwestern part of the state. In contrast, 16 out of the 155 strategic reservoirs (approx. 10%) have an average NRMSE above 100%. For the historic model experiment, we also calculate and map the KGEkm for three forecast horizons (Fig. 9d, e and f). Reservoirs with low NRMSE tend to perform well also according to the KGEkm. With regard to the prediction horizon January to June, 77 out of the 155 strategic reservoirs (approx.

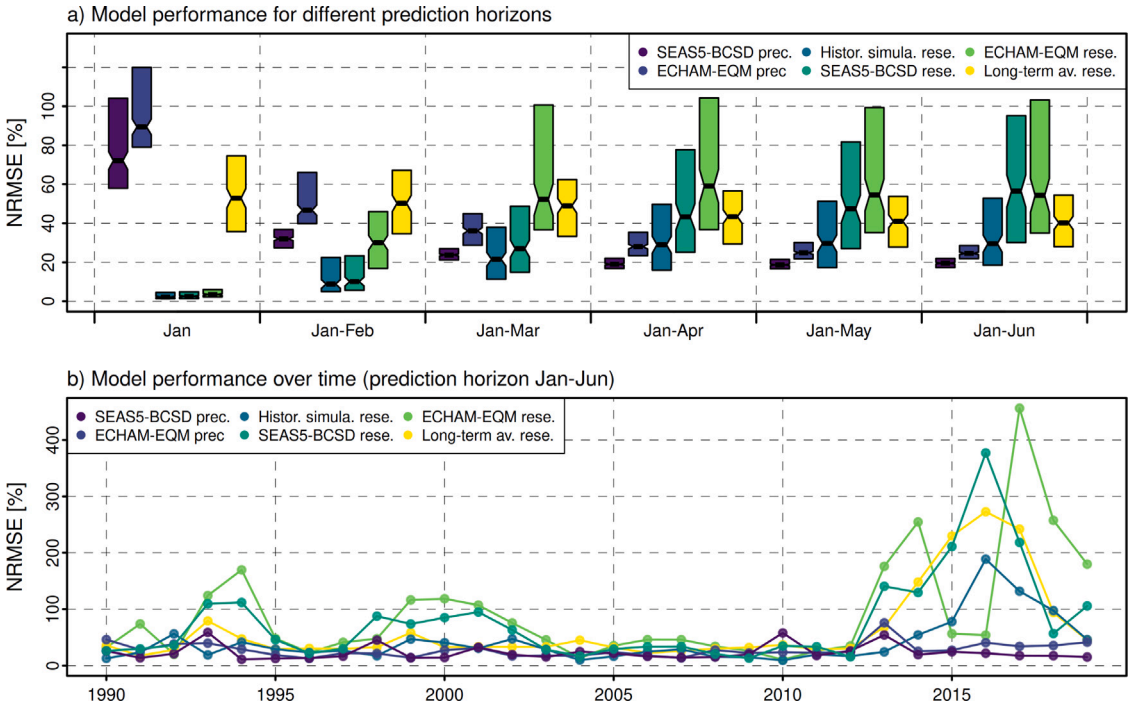

Fig. 7. Hydro-climatological modeling chain assessing the average NRMSE of cumulative precipitation (prec) and reservoir volumes (rese) for the period 1990–2019 for different prediction horizons (a) and on a yearly basis for the prediction horizon January to June (b) for precipitation based on SEAS5 and ECHAM data, reservoir simulations based on observations, SEAS5 and ECHAM data and long-term averages of volume observations.

50%) have a KGEkm higher than 0.4. Also the KGEkm values indicate that the hydrological model is not able to capture the storage dynamic for certain strategic reservoirs.

A simple benchmark for the evaluation of the hydrological model, is the long-term average of in-situ reservoir volume observations as model prediction. The usage of the long-term average of reservoir volume observations as prediction, results in a median average NRMSE for all strategic reservoirs of 40.22% for the prediction horizon January to June (Fig. 7a). The performance of both historic simulations based on meteorological observations and long-term averages of volume observations seem fairly constant in the time frame 1990 to 2012 (Fig. 7b). After the year 2012, which represents the onset of a severe multi-year drought in the region, NRMSE values increase.

With regard to hindcast simulations for the time frame 1990 to 2019 and the prediction horizon January to June, our results point at a median average NRMSE for all strategic reservoirs of 54.28% for the ECHAM hindcast simulations and 56.50% for the SEAS5 hindcast experiment (Fig. 7a). Our results suggest that reservoirs with weak model performance during historic simulations based on observations (Fig. 8a) also perform weakly in hindcast mode (Fig. 8e). Due to the assimilation of observed values at the beginning of the hindcast simulation, we observe a better model performance with short prediction horizons (Fig. 7a). In general, the results from the hindcast experiments (Fig. 8b,e) suggest a superposition of errors from the climate models (Fig. 8c,f) with errors origination from uncertainties within the hydrological model (Fig. 8a).

3.2.3. Seasonal forecast simulations

In addition to hindcast simulations, we present seasonal forecast runs with recent ECHAM data for the strategic reservoir Trussu (id = 122). The annual rainfall sums for the upstream watershed, which base on interpolated station observations, point at the large inter-annual variability of rainfall amounts in the region (Fig. 10a). The case of Trussu illustrates the fact that a succession of dry years (e.g. 2012–2019) can result in the desiccation of a strategic reservoir (Fig. 10b). Several years with above-average rainfall are required to re-fill the reservoir to pre-drought levels.

The ECHAM forecast of January 2019 strongly overestimates the actual rainfall sums (Fig. 11a). All twenty forecast members result in higher rainfall amounts than were finally observed. Due to the little amount of rainfall in the sub-basin upstream of the strategic reservoir, only little to no inflow to the strategic reservoir occurs in this year (Figs. 10b and 11e). Such an overestimation in the forecast might result in an overconsumption of water driven by the expectation of a replenishment that, however, does not occur. On the other hand, an underestimation in the forecast might lead to unnecessary restraints and untapped potentials. In the year 2020, a selection of ECHAM members can capture the observed rainfall amounts (Fig. 11b). The average of all members still is well above the actually observed values. In turn, hydrological simulations driven by those forecasts overestimate the water available in the reservoir (Fig. 11f). In the period January to June in the year 2021, more rainfall than predicted is observed. The reservoir

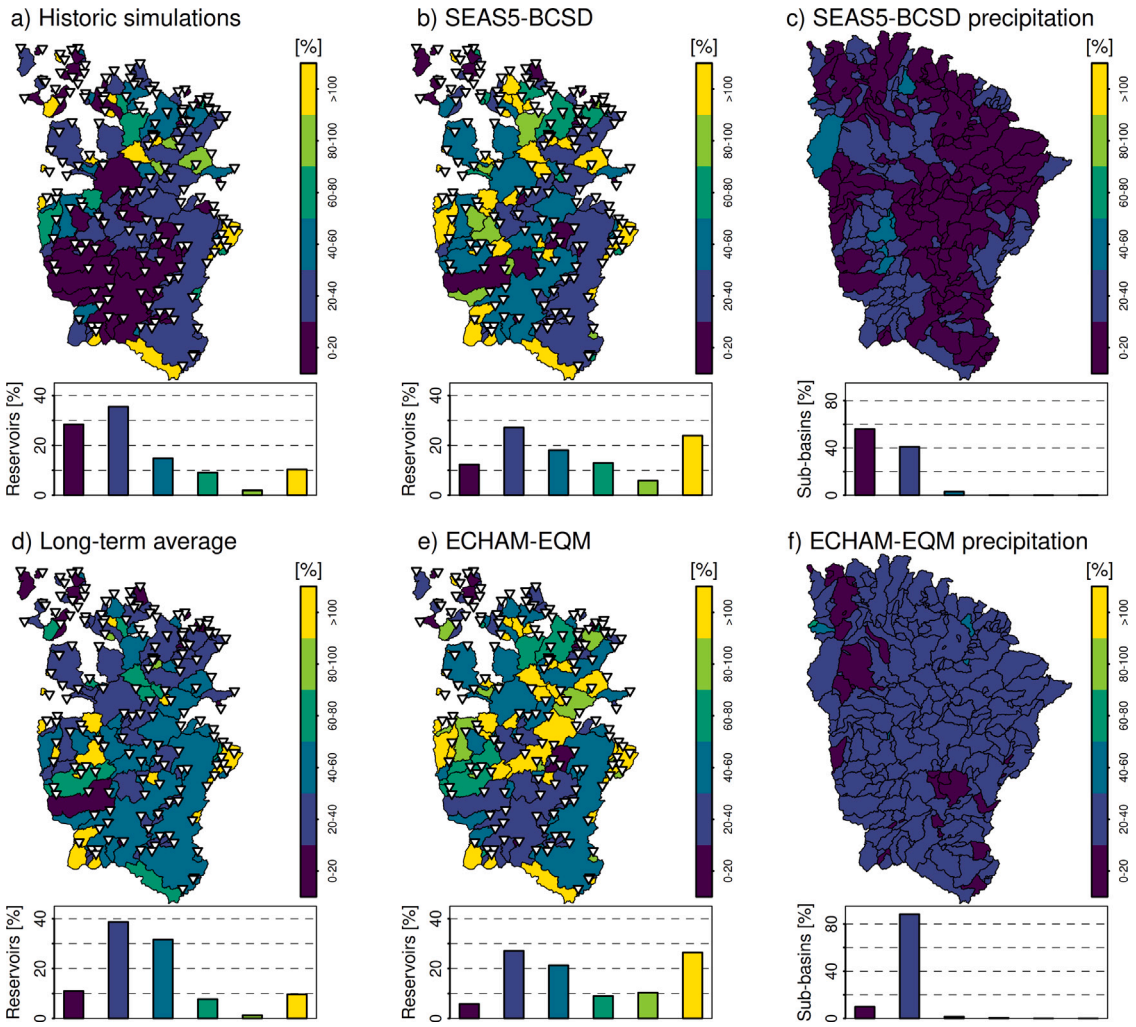

Fig. 8. Performance evaluation of the hydro-climatological modeling chain assessing the average NRMSE for the time frame 1990–2019 and prediction horizon January to June for strategic reservoirs (a, b, d, and e) and sub-basins (c and f) for volume simulations based on historic observations (a), volume simulations based on SEAS5 data (b), precipitation based on SEAS5 data (c), long-term averages of volume observations (d), volume simulations based on ECHAM hindcast data (e), precipitation based on ECHAM data (f). The frequency of reservoirs/sub-basins within one of the six performance classes is indicated in bar plots in the lower part of the plot panels.

volume slightly increases in comparison to the previous year (Figs. 10c and 11g). The year 2022 represents the year with the most rainfall in the watershed (i.e. 838 mm) since the year 2011 (919 mm). In comparison, the cumulative precipitation predicted is 949 mm (Fig. 11d). The hydrological model predicts a considerable earlier and stronger filling of the reservoir than observed (Fig. 11h).

4. Discussion

4.1. Monitoring reservoirs from space

4.1.1. Area-volume curves

The detected underestimation of maximum storage volumes may be due to the generally lower maximum extents of our remotely sensed reservoir characteristics as compared to the official COGERH data. However, our AV-curves also indicate lower water volumes at lower water levels. These discrepancies between the remotely sensed reservoir bathymetries assessed in this study and the official data on reservoir characteristics are an important result. Some of the original AV-curves data back to the 1990s, and since then sediment deposition, or the increasing spread of macrophytes may have changed the reservoirs geometry and thus the AV-ratios.

To account for the influence of the recording date of TanDEM-X data, one may also use scenes from different years and/or the wet season within a multi-year drought period to obtain AV-curves. This would mean that several curves for one and the same

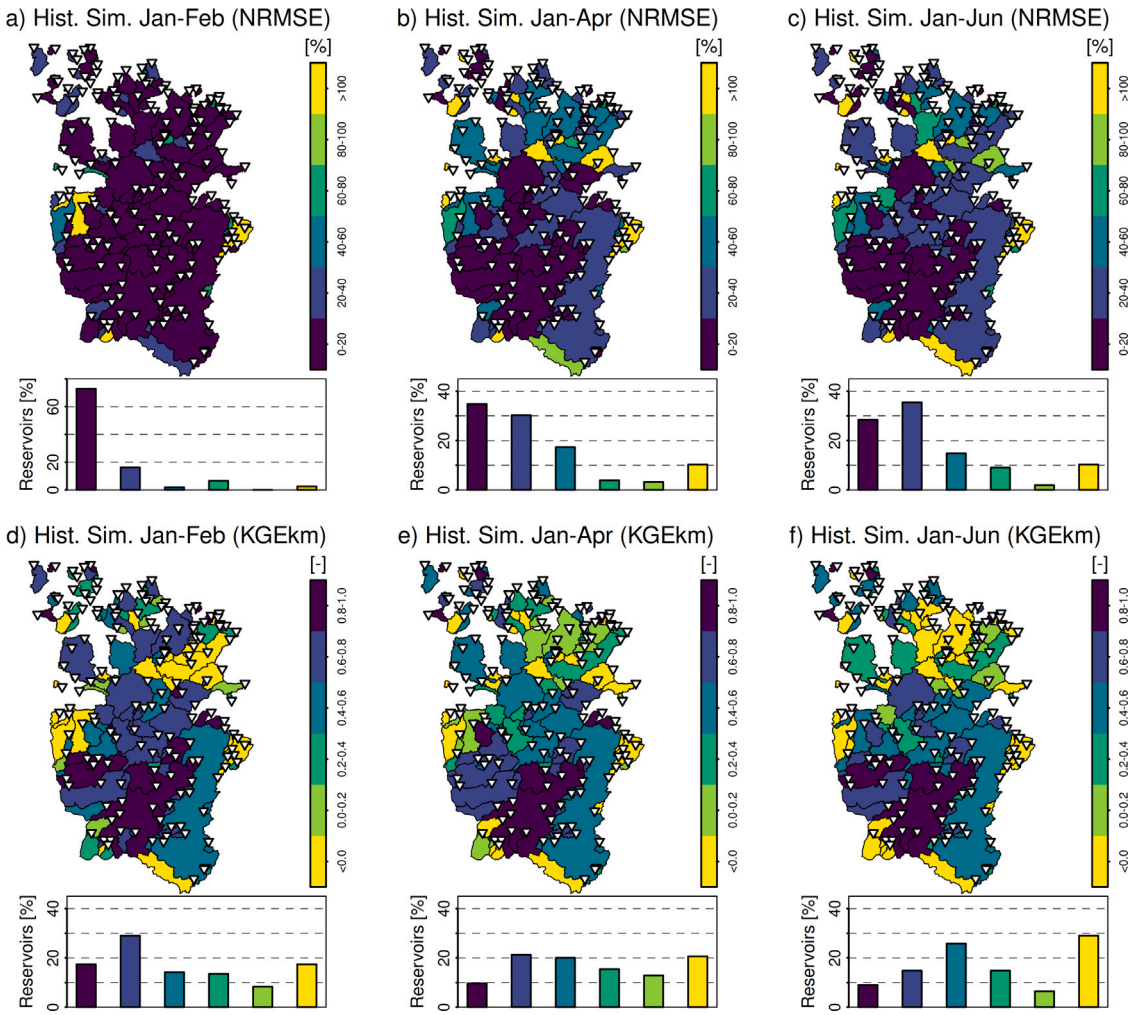

Fig. 9. Performance evaluation of the historic model runs assessing the average NRMSE and KGEkm for the time frame 1990–2019 for the three prediction horizons January to February (a), January to April (b) and January to June (c). The frequency of reservoirs within one the six performance classes is indicated in bar plots in the lower part of the plot panels.

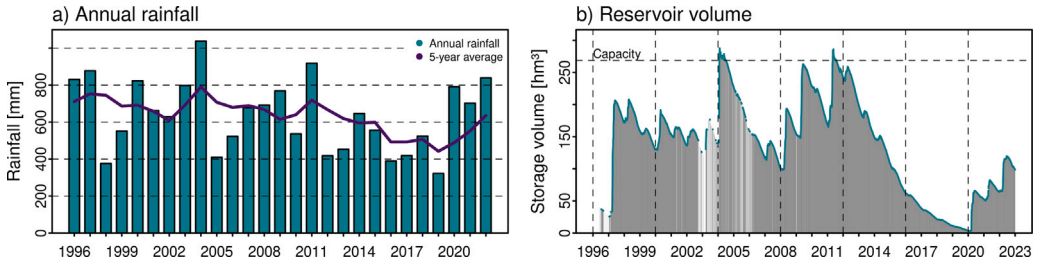

Fig. 10. Annual rainfall amounts in the upstream watershed with right-aligned 5-year moving average (a) and in-situ observed volumes (b) for the strategic reservoir Trussu (id = 122).

reservoir would be available (expressing the uncertainty of this data), and that more reservoirs in Ceará would be covered. The latter would mean that more AV-curves can be directly derived and less regionalization is required.

The comparison with the result of Zhang et al. (2016) suggests that their DEMs show a better accuracy compared to the DEMs generated in this study. However, in contrast to the cited study, we did not use ground-trutz data, i.e. ground GPS data specifically collected for the study (Zhang et al., 2016). Given the large amount of reservoirs and the large size of the study area, the collection of additional ground-truth information and manual parameter optimization was not possible.

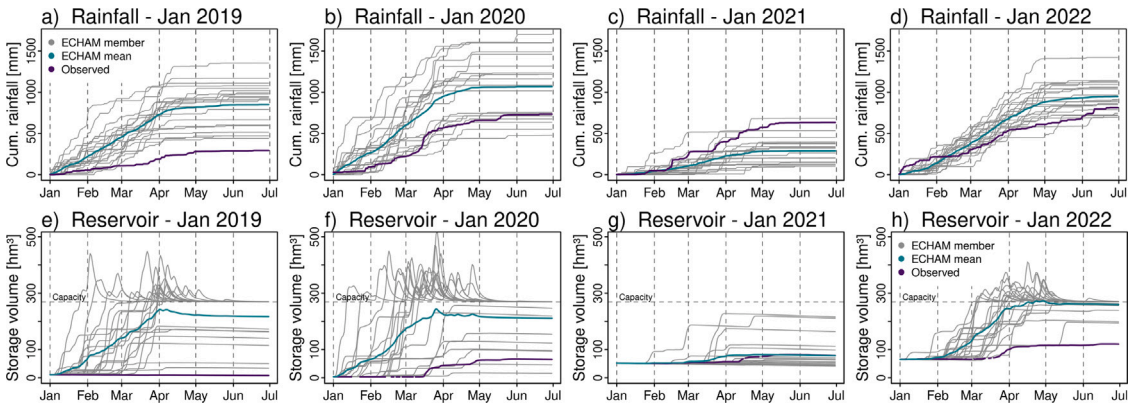

Fig. 11. Cumulative rainfall and reservoir volumes observed and simulated based on ECHAM forecast runs from January 2019, 2020, 2021 and 2022 for the strategic reservoir Trussu (id = 122), which has been constructed in 1996.

The bathymetric data generated in this work represents the largest inventory of such information for the region and exceeds older inventories (Li et al., 2020; Zhang et al., 2021) by far. Particular uncertainties remain with regard to the quality of AV-curves for small and medium reservoirs since the small sample size of 34 strategic reservoirs may not properly represent the state and the dynamics of the more than 50 000 reservoirs in Ceará. Furthermore, one must be aware of the general uncertainties for the assessment of small and medium reservoirs, be it because of sediment deposition (Bronstert et al., 2014; de Araújo et al., 2023), spreading macrophytes (Coelho et al., 2017) or that they were not really empty during the recording date of the selected TanDEM-X scenes. Nevertheless, despite these uncertainties, the data set generated here provides new state-wide information on AV-curves for reservoirs with little to no information so far.

4.1.2. Water surface detection

The Sentinel-1 based water surface detection is less uncertain than the quality of the TanDEM-X derived AV-curves. Still, the derived data shows the same pattern of underestimation as the AV-curves if compared to the COGERH data, which generally shows larger maximum storage capacities. We have mentioned possible reasons for this discrepancy earlier. An additional and independent evaluation of the detected water masks could be a comparison against optical remote sensing data as employed by Markert et al. (2020) and Mayer et al. (2021).

4.2. Hydrological simulations

4.2.1. Model parameterization

We conduct the hillslope-based landscape discretization once for the entire state of Ceará. This results in one common data base for all regions with the same underlying landscape units and terrain components. An alternative approach would be the application of these discretization algorithms for each region individually. This might lead to a better local representation of the terrain and hydrological characteristics and in turn potentially result in better modeling results.

Another aspect with regard to the landscape discretization is the definition of strategic reservoirs, since there are differences between the model assumptions and the view of state water management authorities. Within the model, the most important criteria to define strategic reservoirs are the maximum reservoir storage volume and the importance for the water availability on a regional scale. In the "real world" of water management, also other and more local criteria are considered and also smaller (headwater) reservoirs with rather small storage volumes are considered strategic. Thus, the explicit representation of small reservoirs in the model may result into upstream sub-basins with very small catchment areas, which differ strongly from a typical area of a sub-basin. In contrast, there are large reservoirs, which are officially not termed strategic, but might be rather relevant for water supply, and thus deserve explicit consideration.

Furthermore, the rather generic reservoir-cascade scheme implemented in WASA-SED cannot represent all variations of the actual reservoir network conditions (Güntner and Bronstert, 2004). The applied concept for a reservoir cascade from smaller reservoirs to bigger ones might be an oversimplification. Further cascade as well as parallel structures within the reservoir networks might be more appropriate (Rabelo et al., 2021, 2022). To account for the continuous changes in the reservoir network due to the construction (and removal) of reservoirs, WASA-SED can simulate each year with a different amount of reservoirs in the previously defined classes. Further research is required to harness new insights into recent changes in reservoir networks and filling levels acquired in this study.

Several strategic reservoirs in Ceará are subject to inter-basin water transfer. For a more accurate forecast of water volumes in reservoirs subject to such inter-basin transfer, the amount of water transferred needs to be estimated correctly. The incorporation of such inter-basin water transfer is possible in WASA-SED (Voit et al., 2023; Rodrigues Lima et al., 2023), however, was not carried out in the model set-up used in this study. The incorporation of such inter-basin transfer might improve the model performance for

reservoirs whose reservoir dynamics currently are not captured well. We suspect that the lack of inter-basin transfer is an important factor explaining the low model performance for reservoirs in the Metropolitan Region Fortaleza. In general, our results suggest that an extensive and high quality observational data base for such water extractions and intra-basin transfer is required to establish a reliable hydro-climatological modeling chain.

The selection of a multi-reservoir and capacity-weighted calibration approach using positive volume changes in the strategic reservoirs as target variable proved to enable region-specific model calibrations for the entire state of Ceará. The results of the historic simulation experiment, which was conducted to assess the uncertainty related to the hydrological model, point out that further investigations are required to develop region-specific refinements of the presented approach (Fig. 8a). Efforts to include streamflow measurements are currently ongoing. The introduced NRMSE to assess the model performance for different prediction horizons is a metric that can be communicated to and is understood by decision makers and workers on the ground. Due to the high seasonality of the reservoir fillings, the performance assessment using a multi-year time series and a metric such as the Nash–Sutcliffe efficiency (Nash and Sutcliffe, 1970) needs to be interpreted with caution (Schaefli and Gupta, 2007).

The evaluation of the modeling system over time (Fig. 7a) suggest lower model performance during the multi-year drought starting in 2012. In general, we assume that the model performance is better during wet years compared to dry years. Furthermore, we assume that an extreme drought event such as the multi-year drought between 2012 and 2018 might trigger severe modifications of the general hydrological functioning of this region. Such drought-induced changes in hydrological behavior can manifest themselves, for example, in altered soil hydraulic conductivities, reduced vegetation cover, less hydrological connectivity, altered runoff formation processes, and last but not least an "abnormal" water extraction and operation rules of unmonitored reservoirs. Such changed hydro-system dynamics were described, for instance, by Liu et al. (2021) for southeastern Australia and Avanzi et al. (2020) for Mediterranean river systems. Matanó et al. (2024) point at the non-stationarity of catchment characteristics for hydrological extreme conditions and that persistent drought conditions can alter the hydrological response, especially in arid regions. Furthermore, the direct human control on the water fluxes, storages and distribution, which is accomplished by the omnipresent network of reservoirs and distribution canals, is particularly strong in this study area. It seems that the current model set-up cannot capture the changed conditions showing up during the multi-year drought period. Process studies for such semi-arid hydro-climatological conditions are required to obtain better parameterizations capturing non-stationary conditions during and after extreme drought events.

4.2.2. Seasonal forecast

We use EQM to downscale and bias-correct ECHAM seasonal forecast data with regard to the station network in Ceará. In general, the establishment of a workflow to get from ECHAM output to WASA-SED input proved successful. Still, the hindcast experiment shows that an improvement of the meteorological seasonal forecast is essential to lower the overall uncertainty of the modeling chain. Possible improvement could be the adaption of the bias-correction and downscaling procedure of the EQM towards using individual probability distributions for each month instead of one single distribution for the whole rainy season.

The BCSD of the SEAS5 data uses ERA5-Land data as a reference. Our results suggest that the BCSD approach was able to remove model biases and drifts. The usage of the same reference data and the same downscaling approaches for both ECHAM and SEAS5 data can provide further insights in the forecast quality of both systems. Further research is required to evaluate multivariate and deep learning algorithms for bias correction of forecast data in the region (e.g. Bhowmik et al., 2017; Han et al., 2021; Zarei et al., 2021; Wang and Tian, 2022). In the framework of this study, we were able to establish an extensive data base of monthly forecasts from ECHAM and SEAS5 system for Ceará dating back to the 1980s.

4.2.3. Model uncertainty

With regard to the propagation of model uncertainty, we want to focus on the uncertainty of three main components of the hydrological part of the forecasting framework, i.e., the observational data sets, the meteorological seasonal forecast data and the WASA-SED hydrological model set-up for the area of Ceará. All observations are subject to uncertainty. In the case of precipitation data, a major uncertainty is related to the point measurement at the rainfall stations. Even though this network is rather advanced, some rainfall events have probably not bee registered, in particular in the case of high intense but partially limited convective rain storms. Further uncertainties are introduced through the spatial interpolation of the station data to the hydrological sub-basinIn our opinion, the observed rainfall that is used for model evaluation should be considered as an uncertainty-prone estimate itself. Apart from errors at the measuring operation and introduced during pre-processing steps, we also face the change of data availability over time an issue. Individual time series of in-situ reservoir observations and meteorological observations, for example, have very different length depending on the construction of the corresponding measurement site. Hence, the input data as well as the calculation of the evaluation metrics rest on a time-varying data base.

Our results indicate that the uncertainty coming from the meteorological seasonal forecast systems are in the same order of magnitude than the uncertainty in historic hydrological simulations. Furthermore, our hindcast experiments indicate that in the framework of the seasonal hydrological forecast system, the uncertainties stemming from the different components superimpose. In the long term, further advancements in all segments are required to reduce the overall uncertainty and thus lead to a higher reliability of hydro-meteorological seasonal forecast system for such a large semi-arid region.

5. Conclusion

In this study, we developed a hydrological monitoring and forecasting system for the state of Ceará (Brazil) integrating satellite-based monitoring of reservoir water storage, bias-corrected seasonal weather forecasts and hydrological modeling. The results from historic, hindcast and forecast experiments support current efforts in the region to establish high-quality hydro-meteorological forecast services.

The hydrological model WASA-SED was used to simulate the dynamics of 155 strategic as well as more than 50 000 small to medium sized reservoirs in the region. The hillslope-, soil- and vegetation-based landscape discretization using the LUMP algorithms allowed for the preservation of the landscape variability in the model. In-situ and satellite-based observations of reservoir fillings have been assimilated into the hydrological simulations. To our knowledge, it is the first time that such an integrated monitoring and modeling system has been successfully established in a semi-arid region as large as Ceará. Our system can be considered a blueprint for similar regions of the world.

In combination with the new set of bathymetries and AV-curves derived from TanDEM-X data, the Sentinel-1 based monitoring of water surfaces allowed for state-wide storage volume estimations for all reservoirs including those for which previously no information was available at all. With regard to forecast data, we collect and bias-correct data from ECHAM and SEAS5 seasonal forecasting systems. These data sets can form the basis for future investigation with regard to seasonal forecasting in Ceará and regions with similar hydro-climatological conditions.

Our model experiments and uncertainty assessment point at the difficulty and complexity of providing serviceable seasonal hydrological forecasts at such a large spatial domain under the particular hydrological conditions of a semi-arid climate. The superposition of uncertainties of the different components along the modeling chain, including uncertainties stemming from meteorological observations, meteorological seasonal forecasts and structural and parameter uncertainties of the hydrological model reduce the reliability of the simulations. Furthermore, results indicate a change in the hydrological behavior during the multi-year drought starting in 2012. We have identified some possible options of reducing these uncertainties. Efforts are currently being made to further test and improve the developed integrated framework as part of the operational services at FUNCEME.

CRediT authorship contribution statement

Erwin Rottler: Writing – review & editing, Writing – original draft, Visualization, Validation, Software, Project administration, Conceptualization. **Martin Schüttig:** Writing – review & editing, Visualization, Validation, Methodology. **Axel Bronstert:** Writing – review & editing, Project administration, Funding acquisition, Conceptualization. **Alyson Brayner Sousa Estácio:** Writing – review & editing, Validation, Methodology, Data curation. **Renan Vieira Rocha:** Writing – review & editing, Validation, Methodology, Data curation. **Valdenor Nilo de Carvalho Junior:** Writing – review & editing, Validation, Data curation. **Clecia Cristina Barbosa Guimarães:** Writing – review & editing, Validation, Methodology, Data curation. **Eduardo Sávio P.R. Martins:** Writing – review & editing, Validation, Methodology, Data curation. **Christof Lorenz:** Writing – review & editing, Validation, Methodology, Data curation. **Klaus Vormoor:** Writing – review & editing, Writing – original draft, Visualization, Validation, Project administration, Methodology, Conceptualization.

Data and code availability

Data and scripts used in the study can be obtained upon reasonable request from the authors. Sample data and scripts for the determination of AV-curves, watermask detection, LUMP application as well as model calibration are available at: https://doi.org/10.23728/b2share.56600e085b314dac89931068d8954222

Funding

This project was supported by funds from the World Bank, United States in the framework of the ‘Project to Support the Improvement of Water Security and Strengthen Intelligence in Public Management in the State of Ceará’ part ot the ‘Investment Project Financing - IPF’.

Declaration of competing interest

The authors declare the following financial interests/personal relationships which may be considered as potential competing interests: Erwin Rottler reports financial support was provided by World Bank. Klaus Vormoor reports financial support was provided by World Bank. Martin Schuettig reports financial support was provided by World Bank. Axel Bronstert reports financial support was provided by World Bank. If there are other authors, they declare that they have no known competing financial interests or personal relationships that could have appeared to influence the work reported in this paper.

Acknowledgments

We acknowledge the German Aerospace Centre (DLR) for the provision of the TanDEM-X CoSSC data, the ECMWF for providing SEAS5 data, Copernicus and ESA for the provision of data from the Sentinel-1 mission and COGERH for providing data related to the strategic reservoirs. José Miguel Delgado is thanked for his valuable contribution to the research idea and research design. We thank the entire FUNCEME team for the provision of data and their support on-site and during the numerous online discussion.

References

Avanzi, F., Rungee, J., Maurer, T., Bales, R., Ma, Q., Glaser, S., Conklin, M., 2020. Climate elasticity of evapotranspiration shifts the water balance of mediterranean climates during multi-year droughts. Hydrol. Earth Syst. Sci. 24 (9), 4317–4337. http://dx.doi.org/10.5194/hess-24-4317-2020.

Bacalhau, J.R., Ribeiro Neto, A., Crétaux, J.-F., Bergé-Nguyen, M., Moreira, D.M., 2022. Bathymetry of reservoirs using altimetric data associated to optical images. Adv. Space Res. 69 (11), 4098–4110. http://dx.doi.org/10.1016/j.asr.2022.03.011.

Bhowmik, R.D., Sankarasubramanian, A., Sinha, T., Patskoski, J., Mahinthakumar, G., Kunkel, K.E., 2017. Multivariate downscaling approach preserving cross correlations across climate variables for projecting hydrologic fluxes. J. Hydrometeorol. 18 (8), 2187–2205. http://dx.doi.org/10.1175/JHM-D-16-0160.1.

Borne, M., Lorenz, C., Portele, T.C., Martins, E.S.P., das Chagas Vasconcelos Junior, F., Kunstmann, H., 2022. Seasonal sub-basin-scale runoff predictions: A regional hydrometeorological ensemble Kalman filter framework using global datasets. J. Hydrol.: Reg. Stud. 42, 101146. http://dx.doi.org/10.1016/j.ejrh.2022.101146.

Bronstert, A., de Araújo, J.-C., Batalla, R.J., Costa, A.C., Delgado, J.M., Francke, T., Foerster, S., Guentner, A., López-Tarazón, J.A., Mamede, G.L., et al., 2014. Process-based modelling of erosion, sediment transport and reservoir siltation in mesoscale semi-arid catchments. J. Soils Sediments 14, 2001–2018. http://dx.doi.org/10.1007/s11368-014-0994-1.

Bürger, G., 2020. A seamless filter for daily to seasonal forecasts, with applications to Iran and Brazil. Q. J. R. Meteorol. Soc. 146 (726), 240–253. http://dx.doi.org/10.1002/qj.3670.

Campos, J.N.B., Studart, T.M.C., 2000. An historical perspective on the administration of water in Brazil. Water Int. 25 (1), 148–156. http://dx.doi.org/10.1080/02508060008686806.

Campos, J.N.B., Studart, T.M.C., 2006. Water management and allocation in semiarid areas of Brazil. Water Int. 31 (1), 31–36. http://dx.doi.org/10.1080/02508060608691912.

Chimeli, A.B., De Souza Filho, F., Holanda, M.C., Petterini, F.C., 2008. Forecasting the impacts of climate variability: lessons from the rainfed corn market in Ceará, Brazil. Environ. Dev. Econ. 13 (2), 201—-227. http://dx.doi.org/10.1017/S1355770X07004172.

Coelho, C., Heim, B., Foerster, S., Brosinsky, A., De Araújo, J.C., 2017. In situ and satellite observation of CDOM and Chlorophyll-a dynamics in small water surface reservoirs in the Brazilian semiarid region. Water 9 (12), http://dx.doi.org/10.3390/w9120913.

Costa, A.C., Estacio, A.B., de Souza Filho, F.d.A., Lima Neto, I.E., 2021. Monthly and seasonal streamflow forecasting of large dryland catchments in Brazil. J. Arid Land 13, 205–223. http://dx.doi.org/10.1007/s40333-021-0097-y.

Crespi, A., Petitta, M., Marson, P., Viel, C., Grigis, L., 2021. Verification and bias adjustment of ECMWF SEAS5 seasonal forecasts over Europe for climate service applications. Climate 9 (12), http://dx.doi.org/10.3390/cli9120181.

de Andrade, E.M., Sena, M.G.T., da Silva, A.G.R., Pereira, F.J.S., Lopes, F.B., 2016. Uncertainties of the rainfall regime in a tropical semi-arid region: the case of the state of Ceará. Rev. Agro@ mbiente Online 10 (2), 88–95.

de Araújo, J.C., Bronstert, A., 2016. A method to assess hydrological drought in semi-arid environments and its application to the Jaguaribe River Basin, Brazil. Water Int. 41 (2), 213–230. http://dx.doi.org/10.1080/02508060.2015.1113077.

de Araújo, J., Landwehr, T., Alencar, P., Paulino, W., 2023. Water management causes increment of reservoir silting and reduction of water yield in the semiarid state of Ceará, Brazil. J. South Am. Earth Sci. 121, 104102. http://dx.doi.org/10.1016/j.jsames.2022.104102.

de Araújo, J.C., Mamede, G.L., De Lima, B.P., 2018. Hydrological guidelines for reservoir operation to enhance water governance: Application to the Brazilian semiarid region. Water 10 (11), http://dx.doi.org/10.3390/w10111628.

Delgado, J.M., Voss, S., Bürger, G., Vormoor, K., Murawski, A., Rodrigues Pereira, J.M., Martins, E., Vasconcelos Júnior, F., Francke, T., 2018. Seasonal drought prediction for semiarid northeastern Brazil: verification of six hydro-meteorological forecast products. Hydrol. Earth Syst. Sci. 22 (9), 5041–5056. http://dx.doi.org/10.5194/hess-22-5041-2018.

Duplančić Leder, T., Baučić, M., Leder, N., Gilić, F., 2023. Optical satellite-derived bathymetry: An overview and WoS and scopus bibliometric analysis. Remote Sens. 15 (5), http://dx.doi.org/10.3390/rs15051294.

Ferreira, G.W.S., Reboita, M.S., Drumond, A., 2022. Evaluation of ECMWF-SEAS5 seasonal temperature and precipitation predictions over South America. Climate 10 (9), http://dx.doi.org/10.3390/cli10090128.

Filipponi, F., 2019. Sentinel-1 GRD preprocessing workflow. Proceedings 18, http://dx.doi.org/10.3390/ECRS-3-06201.

Formiga-Johnsson, R.M., Kemper, K., 2005. Institutional and Policy Analysis of River Basin Management: The Jaguaribe River Basin, Ceará, Brazil. World Bank Policy Research Working Paper 3649, URL https://ssrn.com/abstract=757424.

Francke, T., Güntner, A., Mamede, G., Müller, E.N., Bronstert, A., 2008. Automated catena-based discretization of landscapes for the derivation of hydrological modelling units. Int. J. Geogr. Inf. Sci. 22 (2), 111–132. http://dx.doi.org/10.1080/13658810701300873.

Frischkorn, H., Araújo, J.C., Santiago, M.M.F., 2003. Water resources of ceará and piauí. In: Gaiser, T., Krol, M., Frischkorn, H., de Araújo, J.C. (Eds.), Global Change and Regional Impacts: Water Availability and Vulnerability of Ecosystems and Society in the Semiarid Northeast of Brazil. Springer Berlin Heidelberg, Berlin, Heidelberg, pp. 87–94. http://dx.doi.org/10.1007/978-3-642-55659-3_6.

Funceme, 2020. Mapeamento dos Espelhos D'água do Estado do Ceará: área máxima mapeada no período de 2008 a 2020. Internal Report, Fundação Cearense de Meteorologia e Recursos Hídricos, Fortaleza.

Gubler, S., Sedlmeier, K., Bhend, J., Avalos, G., Coelho, C.A.S., Escajadillo, Y., Jacques-Coper, M., Martinez, R., Schwierz, C., de Skansi, M., Spirig, C., 2020. Assessment of ECMWF SEAS5 seasonal forecast performance over South America. Weather Forecast. 35 (2), 561–584. http://dx.doi.org/10.1175/WAF-D-19-0106.1.

Gudmundsson, L., Bremnes, J.B., Haugen, J.E., Engen-Skaugen, T., 2012. Technical note: Downscaling RCM precipitation to the station scale using statistical transformations and a comparison of methods. Hydrol. Earth Syst. Sci. 16 (9), 3383–3390. http://dx.doi.org/10.5194/hess-16-3383-2012.

Güntner, A., 2002. Large-Scale Hydrological Modelling in the Semi-Arid North-East of Brazil. PIK Report No. 77, Institute for Climate Impact Research, Potsdam, Germany.

Güntner, A., Bronstert, A., 2004. Representation of landscape variability and lateral redistribution processes for large-scale hydrological modelling in semi-arid areas. J. Hydrol. 297 (1–4), 136–161. http://dx.doi.org/10.1016/j.jhydrol.2004.04.008.

Gupta, H.V., Kling, H., Yilmaz, K.K., Martinez, G.F., 2009. Decomposition of the mean squared error and NSE performance criteria: Implications for improving hydrological modelling. J. Hydrol. 377 (1), 80–91. http://dx.doi.org/10.1016/j.jhydrol.2009.08.003.

Han, L., Chen, M., Chen, K., Chen, H., Zhang, Y., Lu, B., Song, L., Qin, R., 2021. A deep learning method for bias correction of ECMWF 24–240 h forecasts. Adv. Atmos. Sci. 38 (9), 1444–1459. http://dx.doi.org/10.1007/s00376-021-0215-y.

Hao, Z., Singh, V.P., Xia, Y., 2018. Seasonal drought prediction: Advances, challenges, and future prospects. Rev. Geophys. 56 (1), 108–141. http://dx.doi.org/10.1002/2016RG000549.

Huang, C., Chen, Y., Zhang, S., Wu, J., 2018. Detecting, extracting, and monitoring surface water from space using optical sensors: A review. Rev. Geophys. 56 (2), 333–360. http://dx.doi.org/10.1029/2018RG000598.

Jacomine, P.K.T., Almeida, J.C., Medeiros, L.A.R., 1973. Levantamento exploratorio – reconhecimento de solos do estado do ceará vol.1. DNPEA, DRN-SUDENE, Recife, Brazil.

Jarvis, A., Reuter, H.I., Nelson, A., Guevara, E., 2008. Hole-filled seamless SRTM data V4. International Centre for Tropical Agriculture (CIAT). URL https://srtm.csi.cgiar.org.

Johnson, S.J., Stockdale, T.N., Ferranti, L., Balmaseda, M.A., Molteni, F., Magnusson, L., Tietsche, S., Decremer, D., Weisheimer, A., Balsamo, G., Keeley, S.P.E., Mogensen, K., Zuo, H., Monge-Sanz, B.M., 2019. SEAS5: the new ECMWF seasonal forecast system. Geosci. Model Dev. 12 (3), 1087–1117. http://dx.doi.org/10.5194/gmd-12-1087-2019.

Kneis, D., 2012. Geostat: Utilities for spatial interpolation. URL https://github.com/echse/echse_tools/tree/master/R/packages/geostat. R package version 0.1.

Krieger, G., Moreira, A., Fiedler, H., Hajnsek, I., Werner, M., Younis, M., Zink, M., 2007. TanDEM-X: A satellite formation for high-resolution SAR interferometry. IEEE Trans. Geosci. Remote Sens. 45 (11), 3317–3341. http://dx.doi.org/10.1109/TGRS.2007.900693.

Li, Y., Gao, H., Zhao, G., Tseng, K.-H., 2020. A high-resolution bathymetry dataset for global reservoirs using multi-source satellite imagery and altimetry. Remote Sens. Environ. 244, 111831. http://dx.doi.org/10.1016/j.rse.2020.111831.

Liu, Y., Liu, P., Zhang, L., Zhang, X., Zhang, Y., Cheng, L., 2021. Detecting and attributing drought-induced changes in catchment hydrological behaviours in a southeastern Australia catchment using a data assimilation method. Hydrol. Process. 35 (7), e14289. http://dx.doi.org/10.1002/hyp.14289.

Liu, W., Sun, F., Lim, W.H., Zhang, J., Wang, H., Shiogama, H., Zhang, Y., 2018. Global drought and severe drought-affected populations in 1.5 and 2° C warmer worlds. Earth Syst. Dyn. 9 (1), 267–283. http://dx.doi.org/10.5194/esd-9-267-2018.

Lorenz, C., Portele, T.C., Laux, P., Kunstmann, H., 2021. Bias-corrected and spatially disaggregated seasonal forecasts: a long-term reference forecast product for the water sector in semi-arid regions. Earth Syst. Sci. Data 13 (6), 2701–2722. http://dx.doi.org/10.5194/essd-13-2701-2021.

Mady, B., Lehmann, P., Gorelick, S.M., Or, D., 2020. Distribution of small seasonal reservoirs in semi-arid regions and associated evaporative losses. Environ. Res. Commun. 2 (6), 061002. http://dx.doi.org/10.1088/2515-7620/ab92af.

Mamede, G.L., Araújo, N.A., Schneider, C.M., de Araújo, J.C., Herrmann, H.J., 2012. Overspill avalanching in a dense reservoir network. Proc. Natl. Acad. Sci. 109 (19), 7191–7195. http://dx.doi.org/10.1073/pnas.1200398109.

Marengo, J.A., Bernasconi, M., 2015. Regional differences in aridity/drought conditions over Northeast Brazil: present state and future projections. Clim. Change 129, 103–115. http://dx.doi.org/10.1007/s10584-014-1310-1.

Marengo, J.A., Galdos, M.V., Challinor, A., Cunha, A.P., Marin, F.R., Vianna, M.d.S., Alvala, R.C.S., Alves, L.M., Moraes, O.L., Bender, F., 2022. Drought in Northeast Brazil: A review of agricultural and policy adaptation options for food security. Clim. Resil. Sustain. 1 (1), e17. http://dx.doi.org/10.1002/cli2.17.

Marengo, J.A., Torres, R.R., Alves, L.M., 2017. Drought in Northeast Brazil—past, present, and future. Theor. Appl. Climatol. 129, 1189–1200. http://dx.doi.org/10.1007/s00704-016-1840-8.

Markert, K.N., Markert, A.M., Mayer, T., Nauman, C., Haag, A., Poortinga, A., Bhandari, B., Thwal, N.S., Kunlamai, T., Chishtie, F., Kwant, M., Phongsapan, K., Clinton, N., Towashiraporn, P., Saah, D., 2020. Comparing sentinel-1 surface water mapping algorithms and radiometric terrain correction processing in southeast Asia utilizing google earth engine. Remote Sens. 12 (15), http://dx.doi.org/10.3390/rs12152469.

Matanó, A., Hamed, R., Brunner, M.I., Barendrecht, M.H., Van Loon, A.F., 2024. Drought decreases streamflow response to precipitation especially in arid regions. EGUsphere 2024, 1–27. http://dx.doi.org/10.5194/egusphere-2024-2715.

Mayer, T., Poortinga, A., Bhandari, B., Nicolau, A.P., Markert, K., Thwal, N.S., Markert, A., Haag, A., Kilbride, J., Chishtie, F., Wadhwa, A., Clinton, N., Saah, D., 2021. Deep learning approach for Sentinel-1 surface water mapping leveraging Google Earth Engine. ISPRS Open J. Photogramm. Remote Sens. 2, 100005. http://dx.doi.org/10.1016/j.ophoto.2021.100005.

Meira Neto, A.A., Medeiros, P., de Araújo, J.C., Pereira, B., Sivapalan, M., 2024. Evolution of drought mitigation and water security through 100 years of reservoir expansion in semi-arid Brazil. Water Resour. Res. 60 (9), e2023WR036411. http://dx.doi.org/10.1029/2023WR036411.

Molle, F., 1994. Geometria dos pequenos açudes. Sudene, Recife, Brazil..

Mueller, E.N., Güntner, A., Francke, T., Mamede, G., 2010. Modelling sediment export, retention and reservoir sedimentation in drylands with the WASA-SED model. Geosci. Model Dev. 3 (1), 275–291. http://dx.doi.org/10.5194/gmd-3-275-2010.

Nash, J., Sutcliffe, J., 1970. River flow forecasting through conceptual models part I — A discussion of principles. J. Hydrol. 10 (3), 282–290. http://dx.doi.org/10.1016/0022-1694(70)90255-6.

Naumann, G., Cammalleri, C., Mentaschi, L., Feyen, L., 2021. Increased economic drought impacts in Europe with anthropogenic warming. Nature Clim. Change 11 (6), 485–491. http://dx.doi.org/10.1038/s41558-021-01044-3.

van Oel, P.R., Krol, M.S., Hoekstra, A.Y., de Araujo, J.C.N., 2008. The impact of upstream water abstractions on reservoir yield: the case of the Orós Reservoir in Brazil. Hydrol. Sci. J. 53 (4), 857–867. http://dx.doi.org/10.1623/hysj.53.4.857.

Otsu, N., 1979. A threshold selection method from gray-level histograms. IEEE Trans. Syst. Man Cybern. 9 (1), 62–66. http://dx.doi.org/10.1109/TSMC.1979.4310076.

Pereira, B., Medeiros, P., Francke, T., Ramalho, G., Foerster, S., Araújo, J.C.D., 2019. Assessment of the geometry and volumes of small surface water reservoirs by remote sensing in a semi-arid region with high reservoir density. Hydrol. Sci. J. 64 (1), 66–79. http://dx.doi.org/10.1080/02626667.2019.1566727.

Pilz, T., Delgado, J.M., Voss, S., Vormoor, K., Francke, T., Costa, A.C., Martins, E., Bronstert, A., 2019. Seasonal drought prediction for semiarid northeast Brazil: what is the added value of a process-based hydrological model? Hydrol. Earth Syst. Sci. 23 (4), 1951–1971. http://dx.doi.org/10.5194/hess-23-1951-2019.

Pilz, T., Francke, T., Bronstert, A., 2017. lumpR 2.0. 0: an r package facilitating landscape discretisation for hillslope-based hydrological models. Geosci. Model Dev. 10 (8), 3001–3021. http://dx.doi.org/10.5194/gmd-2017-17.

Pizarro, A., Jorquera, J., 2024. Advancing objective functions in hydrological modelling: Integrating knowable moments for improved simulation accuracy. J. Hydrol. 634, 131071. http://dx.doi.org/10.1016/j.jhydrol.2024.131071.

Pontes Filho, J.D., Souza Filho, F.d., Martins, E.S.P.R., Studart, T.M.d.C., 2020. Copula-based multivariate frequency analysis of the 2012–2018 drought in Northeast Brazil. Water 12 (3), http://dx.doi.org/10.3390/w12030834.

Portele, T.C., Lorenz, C., Dibrani, B., Laux, P., Bliefernichts, J., Kunstmann, H., 2021. Seasonal forecasts offer economic benefit for hydrological decision making in semi-arid regions. Sci. Rep. 11, 10581. http://dx.doi.org/10.1038/s41598-021-89564-y.

Rabelo, U.P., Costa, A.C., Dietrich, J., Fallah-Mehdipour, E., Van Oel, P., Lima Neto, I.E., 2022. Impact of dense networks of reservoirs on streamflows at dryland catchments. Sustainability 14 (21), http://dx.doi.org/10.3390/su142114117.

Rabelo, U.P., Dietrich, J., Costa, A.C., Simshäuser, M.N., Scholz, F.E., Nguyen, V.T., Lima Neto, I.E., 2021. Representing a dense network of ponds and reservoirs in a semi-distributed dryland catchment model. J. Hydrol. 603, 127103. http://dx.doi.org/10.1016/j.jhydrol.2021.127103.

Raulino, J.B.S., Silveira, C.S., Neto, I.E.L., 2021. Assessment of climate change impacts on hydrology and water quality of large semi-arid reservoirs in Brazil. Hydrol. Sci. J. 66 (8), 1321–1336. http://dx.doi.org/10.1080/02626667.2021.1933491.

Reuter, H.I., Nelson, A., Jarvis, A., 2007. An evaluation of void-filling interpolation methods for SRTM data. Int. J. Geogr. Inf. Sci. 21 (9), 983–1008. http://dx.doi.org/10.1080/13658810601169899.

Rizzoli, P., Martone, M., Gonzalez, C., Wecklich, C., Borla Tridon, D., Bräutigam, B., Bachmann, M., Schulze, D., Fritz, T., Huber, M., Wessel, B., Krieger, G., Zink, M., Moreira, A., 2017. Generation and performance assessment of the global tandem-x digital elevation model. ISPRS J. Photogramm. Remote Sens. 132, 119–139. http://dx.doi.org/10.1016/j.isprsjprs.2017.08.008.

Rodrigues, G.P., Brosinsky, A., Rodrigues, Í.S., Mamede, G.L., de Araújo, J.C., 2024. Impact of reservoir evaporation on future water availability in north-eastern Brazil: a multi-scenario assessment. Hydrol. Earth Syst. Sci. 28 (14), 3243–3260. http://dx.doi.org/10.5194/hess-28-3243-2024.

Rodrigues, I., Costa, C.A.G., Raabe, A., Medeiros, P.H.A., de Araújo, J.C., 2021. Evaporation in Brazilian dryland reservoirs: Spatial variability and impact of riparian vegetation. Sci. Total Environ. 797, 149059. http://dx.doi.org/10.1016/j.scitotenv.2021.149059.

Rodrigues Lima, T.B., Augusto Medeiros, P.H., Mamede, G.L., de Araújo, J.C., 2023. Impact of intensive water use from farm dams on the storage dynamics in strategic reservoirs. Hydrol. Sci. J. 68 (16), 2422–2434. http://dx.doi.org/10.1080/02626667.2023.2272669.

Roeckner, E., Arpe, K., Bengtsson, L., Christoph, M., Claussen, M., Dümenil, L., Esch, M., Giorgetta, M., Schlese, U., Schulzweida, U., 1996. The Atmospheric General Circulation Model ECHAM-4: Model Description and Simulation of Present-Day Climate. MPI-Report 218, Max-Planck-Institut for Meteorologie, URL https://mpimet.mpg.de/fileadmin/publikationen/Reports/MPI-Report_218.pdf.

Rossi, G., Cancelliere, A., 2013. Managing drought risk in water supply systems in Europe: a review. Int. J. Water Resour. Dev. 29 (2), 272–289. http://dx.doi.org/10.1080/07900627.2012.713848.

Schaefli, B., Gupta, H.V., 2007. Do Nash values have value? Hydrol. Process. 21 (15), 2075–2080. http://dx.doi.org/10.1002/hyp.6825.

Shen, H., Tolson, B.A., Mai, J., 2022. Time to update the split-sample approach in hydrological model calibration. Water Resour. Res. 58 (3), e2021WR031523. http://dx.doi.org/10.1029/2021WR031523.

Souza Filho, F.A., Lall, U., 2003. Seasonal to interannual ensemble streamflow forecasts for Ceará, Brazil: Applications of a multivariate, semiparametric algorithm. Water Resour. Res. 39 (11), http://dx.doi.org/10.1029/2002WR001373.

Stockdale, T., Johnson, S., Ferranti, L., Balmaseda, M., Briceag, S., 2018. ECMWF's new long-range forecasting system SEAS5. http://dx.doi.org/10.21957/tsb6n1, URL https://www.ecmwf.int/node/18202.

Sugg, M., Runkle, J., Leeper, R., Bagli, H., Golden, A., Handwerger, L.H., Magee, T., Moreno, C., Reed-Kelly, R., Taylor, M., et al., 2020. A scoping review of drought impacts on health and society in north america. Clim. Change 162, 1177–1195. http://dx.doi.org/10.1007/s10584-020-02848-6.

Sun, L., Li, H., Zebiak, S.E., Moncunill, D.F., Filho, F.D.A.D.S., Moura, A.D., 2006. An operational dynamical downscaling prediction system for nordeste Brazil and the 2002–04 real-time forecast evaluation. J. Clim. 19 (10), 1990–2007. http://dx.doi.org/10.1175/JCLI3715.1.

Tolson, B.A., Shoemaker, C.A., 2007. Dynamically dimensioned search algorithm for computationally efficient watershed model calibration. Water Resour. Res. 43 (1), http://dx.doi.org/10.1029/2005WR004723.

Trenberth, K.E., Dai, A., Van Der Schrier, G., Jones, P.D., Barichivich, J., Briffa, K.R., Sheffield, J., 2014. Global warming and changes in drought. Nature Clim. Change 4 (1), 17–22. http://dx.doi.org/10.1038/nclimate2067.

Vogel, J., Paton, E., Aich, V., Bronstert, A., 2021. Increasing compound warm spells and droughts in the mediterranean basin. Weather Clim. Extremes 32, 100312. http://dx.doi.org/10.1016/j.wace.2021.100312.

Voit, P., Francke, T., Bronstert, A., 2023. Accounting for operational irrigation options in mesoscale hydrological modelling of dryland environments. Hydrol. Sci. J. 68 (5), 670–684. http://dx.doi.org/10.1080/02626667.2023.2187296.

Wang, F., Tian, D., 2022. On deep learning-based bias correction and downscaling of multiple climate models simulations. Clim. Dyn. 59 (11), 3451–3468. http://dx.doi.org/10.1007/s00382-022-06277-2.

Xavier, A.C., Scanlon, B.R., King, C.W., Alves, A.I., 2022. New improved Brazilian daily weather gridded data (1961–2020). Int. J. Climatol. http://dx.doi.org/10.1002/joc.7731.

Yapo, P.O., Gupta, H.V., Sorooshian, S., 1996. Automatic calibration of conceptual rainfall-runoff models: sensitivity to calibration data. J. Hydrol. 181 (1), 23–48. http://dx.doi.org/10.1016/0022-1694(95)02918-4.

Yuan, X., Wang, Y., Ji, P., Wu, P., Sheffield, J., Otkin, J.A., 2023. A global transition to flash droughts under climate change. Science 380 (6641), 187–191. http://dx.doi.org/10.1126/science.abn6301.

Zambrano-Bigiarini, M., 2024. hydroGOF: Goodness-of-fit functions for comparison of simulated and observed hydrological time series. http://dx.doi.org/10.5281/zenodo.839854, URL https://cran.r-project.org/package=hydroGOF. R package version 0.6-0.

Zarei, M., Najarchi, M., Mastouri, R., 2021. Bias correction of global ensemble precipitation forecasts by random forest method. Earth Sci. Inform. 14, 677–689. http://dx.doi.org/10.1007/s12145-021-00577-7.

Zhang, S., Foerster, S., Medeiros, P., de Araújo, J.C., Duan, Z., Bronstert, A., Waske, B., 2021. Mapping regional surface water volume variation in reservoirs in northeastern Brazil during 2009–2017 using high-resolution satellite images. Sci. Total Environ. 789, 147711. http://dx.doi.org/10.1016/j.scitotenv.2021.147711.

Zhang, S., Foerster, S., Medeiros, P., de Araújo, J.C., Motagh, M., Waske, B., 2016. Bathymetric survey of water reservoirs in north-eastern Brazil based on tandem-x satellite data. Sci. Total Environ. 571, 575–593. http://dx.doi.org/10.1016/j.scitotenv.2016.07.024.